STRUCTURAL BIOLOGY

Volume 74 (2018)

Supporting information for article:

Orthorhombic lysozyme crystallization at acidic pH values driven by phosphate binding

Marina Plaza-Garrido, M. Carmen Salinas-Garcia and Ana Camara-Artigas

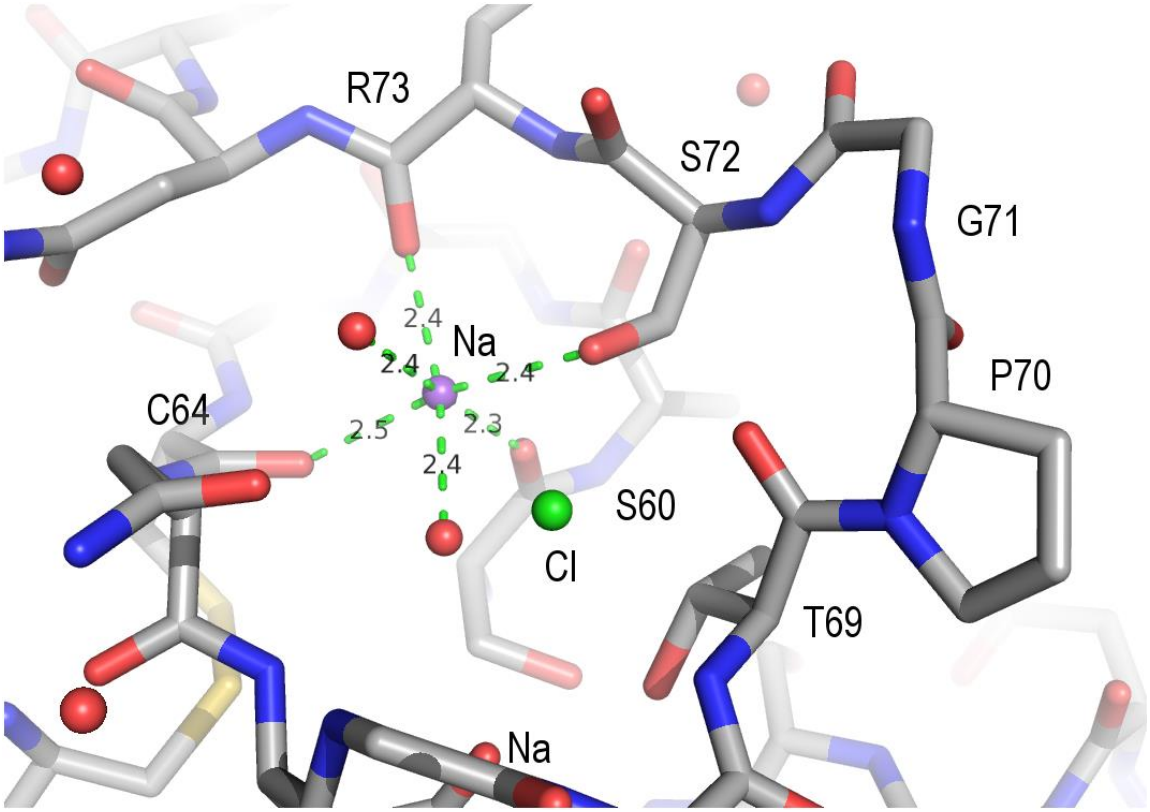
R73
S72
G71
Na
2.4
2.4
2.4
P70
C64
2.5
2.3
2.4
S60
Cl
T69
Na

(A)

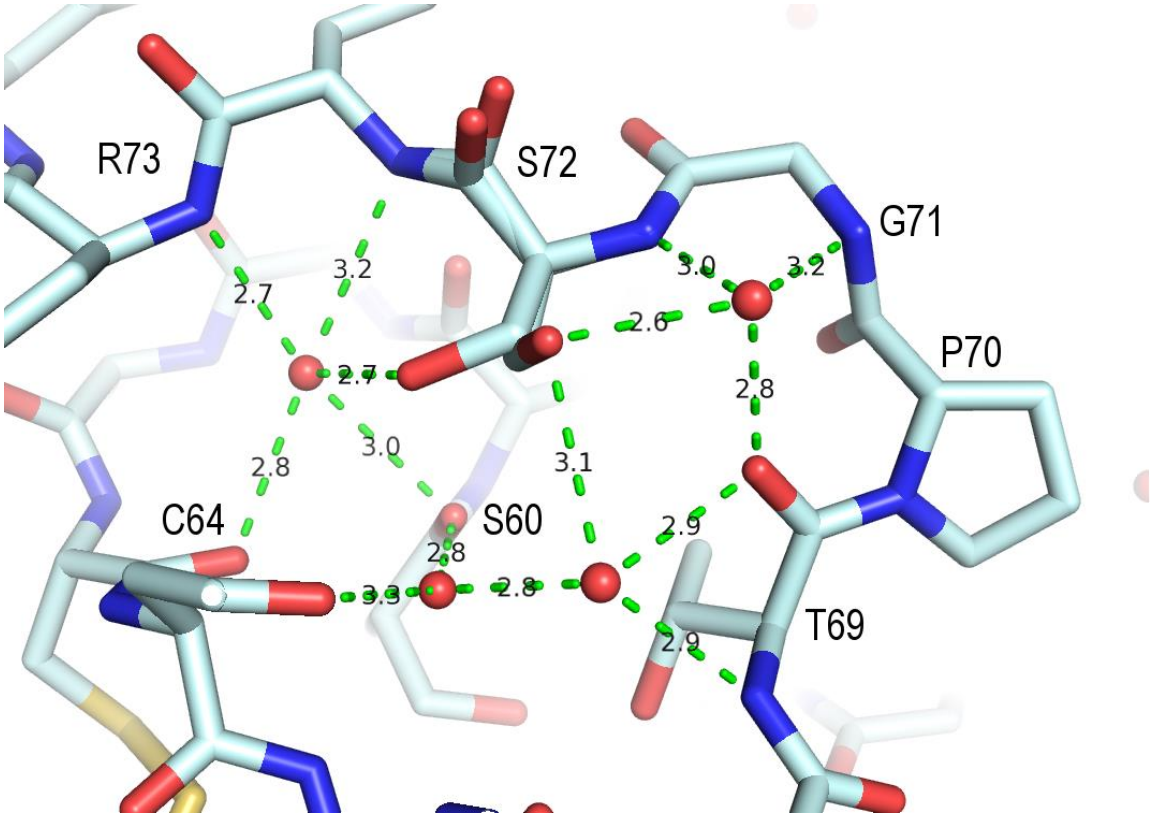
R73
S72
G71
2.7
3.2
3.0
3.2
2.6
P70
2.7
2.8
3.0
3.1
2.8
C64
S60
2.9
2.8
2.8
3.3
T69
2.9

(B)

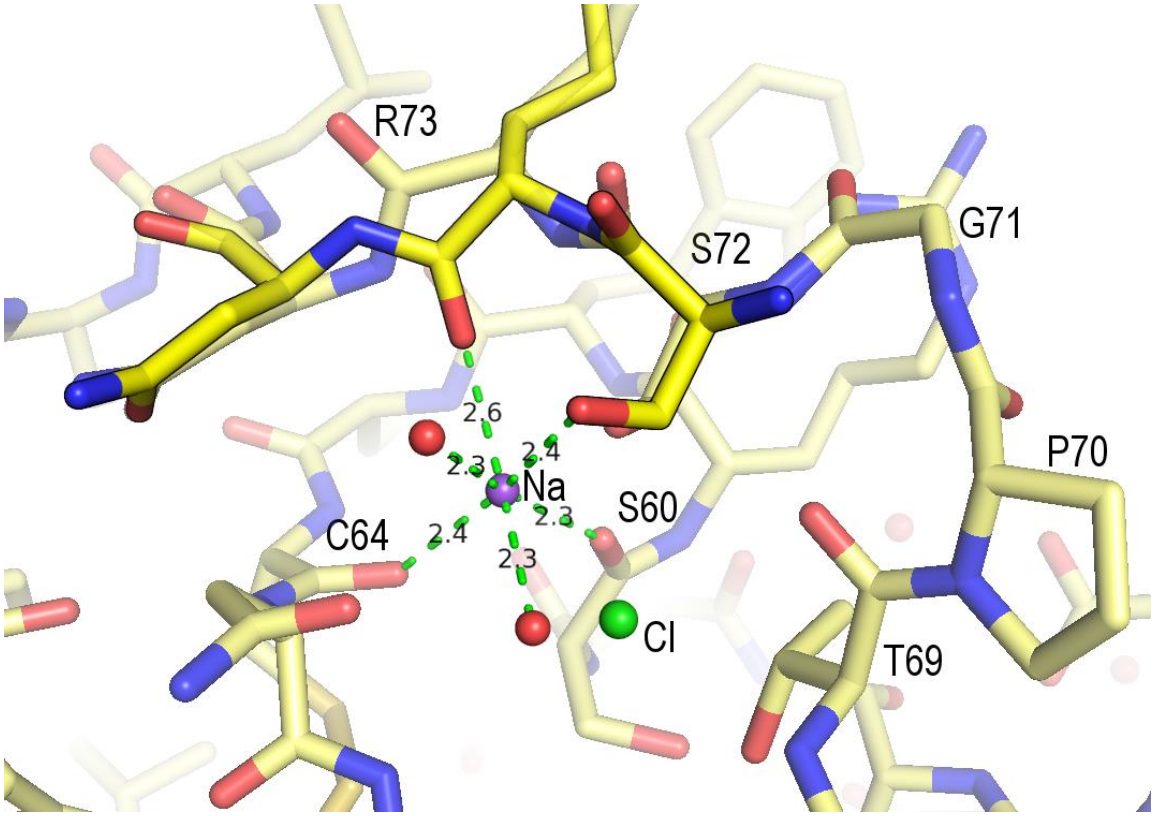
R73
S72
G71
P70
2.6
2.3
2.4
Na
2.3
S60
C64
2.4
2.3
Cl
T69

(C)

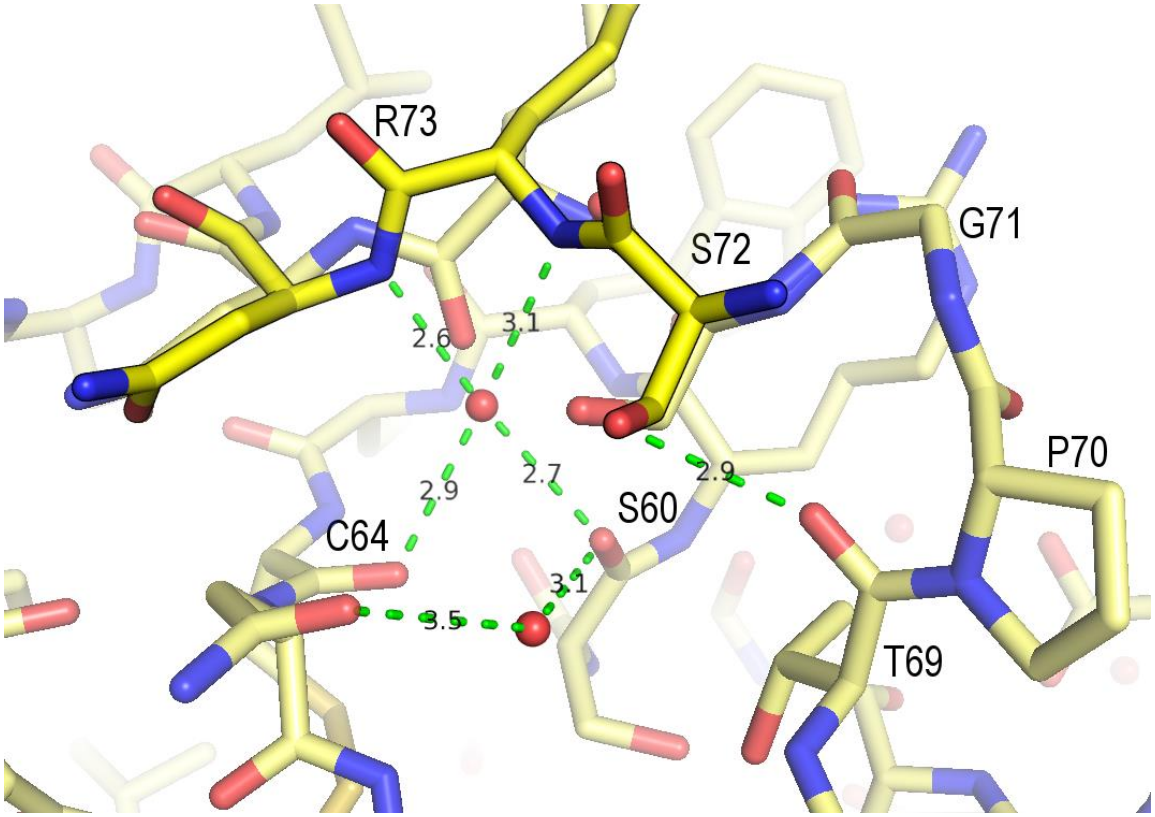
R73
S72
G71
2.6
3.1
P70
2.9
2.7
2.9
S60
C64
3.1
3.5
T69

(D)

Figure S1 Conformational changes that take place upon phosphate binding at the Ser60-Asn74 loop. (A) The tetragonal control structure shows the characteristic sodium ion (purple sphere) bound to the Ser60-Asn74 loop; (B) the orthorhombic structure does not show the sodium ion and instead a water molecule is placed at this position. (C) and (D) show the two alternate conformations of the Ser60-Asn74 loop in the tetragonal crystals grown in the same drop that the orthorhombic crystals. In the first conformation (panel C) bond distances and the coordination are characteristic of the precense of a sodium ion, while in the second conformation (panel D) suggest the presence of a water molecule. Bond distances are shown in green dashed lines.

Table S1 Data collection and processing of lysozyme crystals grown in the presence of sulfate salts

Values for the outer shell are given in parentheses.

PDB entry	6F9Y 10 mM lithium sulfate	6F9X 100 mM lithium sulfate	6F9Z 5 mM ammonium sulfate	6FA0 100 mM ammonium sulfate
Diffraction source	ALBA Xaloc	ALBA Xaloc	ESRF MASSIF-1	ESRF MASSIF-1
Wavelength (Å)	0.97926	0.97926	0.96600	0.96600
Temperature (K)	100	100	100	100
Detector	DECTRIS Pilatus 6M	DECTRIS Pilatus 6M	DECTRIS Pilatus 2M	DECTRIS Pilatus 2M
Crystal-detector distance (mm)	187.510	158.610	101.037	101.037
Rotation range per image (°)	0.10	0.10	0.15	0.15
Total rotation range (°)	360	360	360	360
Exposure time per image (s)	0.098	0.098	0.020	0.020
Space group	$P2_12_12_1$	$P2_12_12_1$	$P2_12_12_1$	$P2_12_12_1$
a, *b*, *c* (Å)	30.13 56.40 73.43	30.09 56.21 73.13	30.01 56.13 72.19	30.09 56.28 73.21
α, β, γ (°)	90.00 90.00 90.00	90.00 90.00 90.00	90.00 90.00 90.00	90.00 90.00 90.00
Mosaicity (°)	0.27	0.67	0.30	0.23
Resolution range (Å)	19.83-1.20	19.77-1.25	19.72 - 1.20	19.79-1.30
Total no. of reflections	175488 (9403)	155400 (3630)	146195 (6960)	123163 (6875)
No. of unique reflections	32486 (1787)	30557 (752)	37901 (1910)	28509 (1504)
Completeness (%)	82.3 (92.9)	86.9 (45.2)	97.5 (97.9)	91.0 (99.6)
Redundancy	5.4 (5.3)	5.1 (4.8)	3.9 (3.6)	4.3 (4.6)
$\langle I/\sigma(I)\rangle$	10.4 (2.3)	12.8 (2.3)	15.5 (2.7)	12.9 (2.1)
R_{meas}	0.078 (0.649)	0.075 (0.705)	0.041 (0.529)	0.055 (0.803)
Overall *B* factor from Wilson plot (Å^2)	11.1	11.9	10.3	11.9

Table S2 Structure solution and refinement of lysozyme crystals grown in the presence of sulfate salts

Values for the outer shell are given in parentheses.

PDB entry	6F9Y 10 mM lithium sulfate	6F9X 100 mM lithium sulfate	6F9Z 5 mM ammonium sulfate	6FA0 100 mM ammonium sulfate
Resolution range (Å)	18.49 - 1.20 (1.24 - 1.20)	19.77 - 1.25 (1.29 - 1.25)	19.72 - 1.2 (1.24 - 1.2)	19.79 – 1.30 (1.35 - 1.3)
Completeness (%)	99.25 (94.14)	86.81 (73.05)	97.16 (98.25)	90.68 (99.61)
σ cutoff	0	0	0	0
No. of reflections, working set	32458 (3613)	30484 (2502	37845 (3756)	28443 (3055)
No. of reflections, test set	1685 (185)	1554 (115)	1923 (191)	1393 (152)
Final R_{cryst}	0.167 (0.257)	0.165 (0.222)	0.157 (0.214)	0.151 (0.228)
Final R_{free}	0.201 (0.313)	0.194 (0.266)	0.180 (0.236)	0.188 (0.238)
No. of non-H atoms	1175	1145	1224	1191
Protein	1002	1012	1035	1013
Ion	6	7	6	6
Water	167	126	183	172
Protein residues	127	127	127	127
R.m.s. deviations				
Bonds (Å)	0.007	0.008	0.012	0.007
Angles (°)	0.91	0.88	1.13	0.89
Average *B* factors (Å^2)	16.13	16.91	17.03	18.08
Protein	14.40	15.63	14.89	16.31
Ion	23.99	32.97	45.03	27.70
Water	26.22	26.27	28.24	28.17
Ramachandran plot				
Most favoured (%)	100.00	99.20	99.20	99.20
Allowed (%)	0.00	0.80	0.80	0.80